Synthetic Seashells: Biomimetic Mineral Nucleation at a Langmuir Monolayer

E. DiMasi[1], V.M. Patel[2], S. Munisamy[2], M. Olszta[2], and L.B. Gower[2]

[1]Brookhaven National Laboratory

[2]University of Florida

Biogenic minerals, formed by living organisms, have properties quite different from those of their inorganic counterparts. Mollusk shells are exemplary biominerals. They are laminates, composed of calcium carbonate, layered with an organic matrix. These materials are structured in a hierarchical manner, in which micron-scale mineral crystallites of controlled shape and orientation are arranged into the larger pattern. Thermodynamically stable and unstable mineral forms can coexist within the same organism, such as for the red abalone (*Haliotis rufescens*) where the exterior of the shell is calcite, but the nacre (mother-of-pearl) layer is composed of crystals of aragonite, a less stable polymorph of calcium carbonate. Nacre is twenty times stronger, in terms of both fracture toughness and specific flexural strength, than inorganic calcium carbonate, due to its laminated structure [1]. Such structural organization on nanometer to micron length scales in synthetic materials would be highly desirable, but this goal has not yet been achieved.

What will it take to "grow" biomimetic (that is, synthetic but bio-inspired) composites? It is clear that the routes to biomineralization are very diverse. For example, certain crustaceans, sponges, and other organisms produce amorphous $CaCO_3$ [2]; abalone shell is microcrystalline; and sea urchin spines are millimeter-long "single crystals" with exceptional alignment across domain boundaries [3]. The complex morphology of biogenic minerals is controlled by two important aspects of their environment during mineralization: the soluble chemical species present, which affect the rate of crystal nucleation and growth, and can also stabilize different crystal faces; and an organic insoluble substrate, which can provide a template for controlled nucleation of specific crystallographic phase or orientation, and acts as a boundary surface for controlling crystal size and shape. The relative importance of the template versus the kinetics is not understood in a general way for biomineralizing systems. One reason for this is that up to now, no in-situ probes on atomic length scales have been available. This means that even when an organic material forming the boundary surface of the biomineral appears to have a good registry with the atomic positions of the crystal faces, it has been very difficult to confirm that the mineral is in fact crystalline at early growth times. If mineralization proceeds first via an amorphous precursor phase, the significance of atomic registry between the template and the final crystal is called into question – the template may still influence crystallization, but the mechanisms for crystallization from a dilute solution are likely to be quite different from those of crystallization from a dense viscous or solid phase. Neither optical microscopy nor electron diffraction can provide the necessary structural information to clarify this problem.

In-situ synchrotron x-ray scattering studies can fill this gap and shed new light on the mechanisms of biomineralization. In this article we describe recent experiments on biomimetic calcium carbonate nucleation. Our model system consists of a liquid subphase and a surfactant monolayer, and provides several advantages. First, the monolayer template's surface charge and lattice spacing may be tuned through careful choice of the organic surfactant, and by the application of surface pressure [4]. Similarly, the ingredients of the subphase can be controlled, and may include the nucleating species along with additional metals or organic molecules thought to influence crystallization. Most importantly, in-situ x-ray scattering allows us to determine the structure of the mineral from its inception as a collection of calcium ions at a monolayer interface, to various bulk phases including macroscopic crystals as well as amorphous thin films. We make use of two complementary techniques. X-ray reflectivity is a sensitive probe of the density profile along the surface normal direction. It is essentially a measurement of interference between x-rays reflecting from boundaries parallel to the surface: in our case, the air-monolayer and monolayer-mineral or monolayer-water interfaces are identified and the density of each region can be modeled and fit to the data [5]. In-plane diffraction measurements are also conducted, with the x-ray beam at grazing incidence to the surface, so that the near-surface region rather than the bulk is probed. This way, the surfactant molecule spacing in the plane as well as the crystallinity of the underlying mineral can be determined. The present work was performed using the Harvard-BNL liquid surface spectrometer at NSLS beamline X22B.

Our experimental conditions are illustrated in the top panel of Figure 1. In all cases, the surfactant is arachidic acid ($CH_3[CH_2]_{18}COOH$): when spread from chloroform solution onto an aqueous subphase and compressed in a Langmuir trough, the molecules stand

up to form a monolayer at the air-water interface. In Scheme (a), the subphase consists of a diluted calcium bicarbonate solution which is acquired by bubbling CO_2 through a suspension of calcite crystals [6]. The deprotonated charged -COOH headgroups are expected to attract a layer of calcium ions (shown as red balls) at the surface. As CO_2 gas escapes from the liquid, the calcium carbonate supersaturation is raised and mineralization proceeds. This system was previously shown to favor the nucleation of oriented vaterite crystals at the surface, as opposed to the calcite that forms in the absence of a monolayer [7]. Schemes (b) and (c) incorporate acidic macromolecules and metal ions, as found in biological environments. In scheme (b), poly(acrylic acid) is added to the supersaturated calcium bicarbonate solution. CO_2 gas escape drives mineralization just as in scheme (a). The polymer (shown as scribbles in the figure) retards calcite crystallization and forces mineralization to proceed via a hydrated amorphous phase [8]. In scheme (c), carbonate supersaturation is controlled in a different way: here, CO_3^{2-} species are supplied by pumping an ammonium carbonate solution into a solution containing Ca^{2+}, along with Mg^{2+} and poly(aspartic acid) as inhibitors. Under some conditions this recipe forces mineralization through a novel *liquid* precursor phase discovered very recently [9]. This polymer-induced liquid-precursor (PILP) process was previously found to form macroscopic amorphous films at stearic acid monolayers on water, and subsequently to crystallize into calcite. An optical micrograph through crossed polarizers, showing a spongy amorphous film along with precursor droplets, is shown in Figure 2. When the precursor is in the liquid form, it can flow into cavities of arbitrary shape, and upon solidification, the crystalline calcite then retains the morphology of the molding space. This process suggests a simple mechanism for “molding” crystalline biogenic minerals to obtain the curved shapes so often observed in nature, and for this reason, understanding the liquid precursor phase is of special interest. Mineralization therefore proceeds through diverse routes, which we summarize schematically in the bottom panel of Figure 1. Figure 1(d) shows the

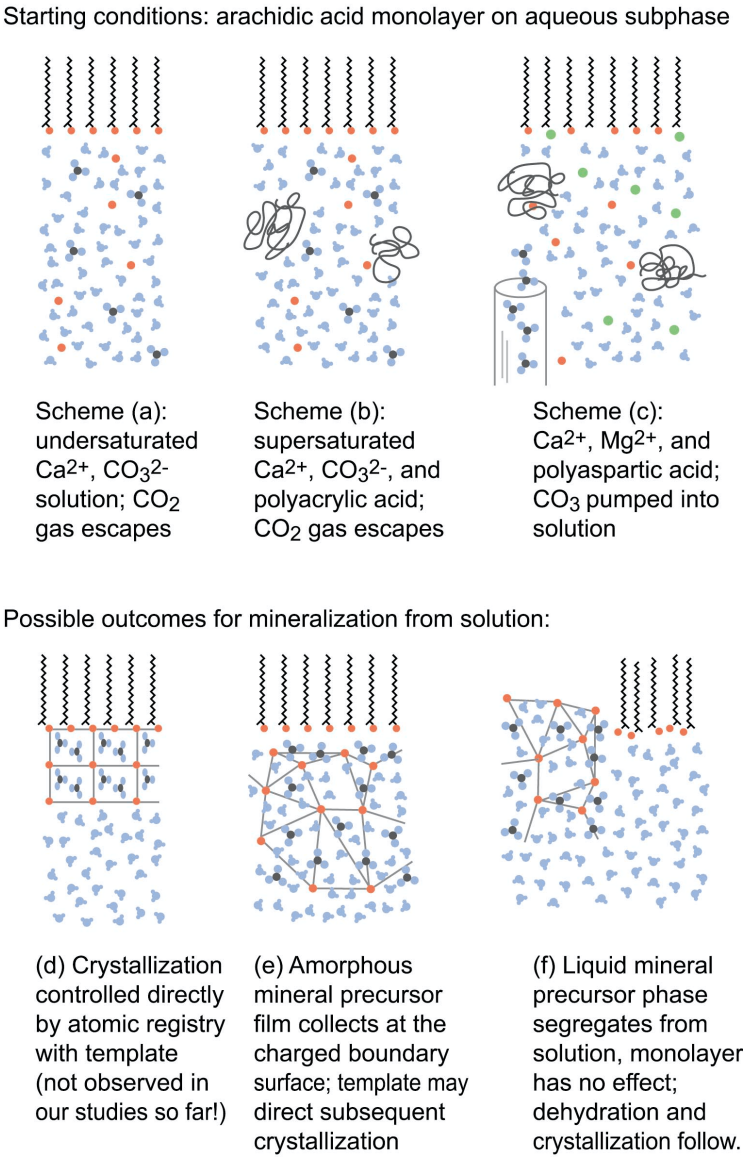

Figure 1. *Top: recipes for mineralization, beginning with a surfactant monolayer (arachidic acid, $CH_3[CH_2]_{18}COOH$) on an aqueous subphase. (a) Supersaturated calcium bicarbonate solution diluted 1:1 with water to produce an undersaturated solution. Carbon dioxide gas escape raises calcium carbonate saturation and promotes mineralization. (b) Supersaturated calcium bicarbonate subphase with polyacrylic acid. (c) Calcium and magnesium cations in solution, carbonate solution pumped into subphase. Bottom: possible outcomes for mineralization. (d) Crystallization controlled directly by atomic registry with monolayer template. (e) Amorphous mineral precursor, collected at charged boundary surface. (f) Mineral precursor nucleates without interacting with monolayer. Red balls, green balls, bent molecules, triangular molecules, and black scribbles represent Ca cations, Mg cations, water molecules, carbonate groups, and soluble polymers respectively.*

template-driven extreme proposed in the literature, where crystal faces align directly at the monolayer template. Figure 1(e) describes an amorphous mineral layer (whether liquid or solid), that simply collects at the charged boundary surface and may subsequently crystallize. We must also be prepared for the situation depicted in Figure 1(f), in which the mineral phase ignores the "template" and nucleates on its own.

X-ray reflectivity is the most effective way of distinguishing the structures described above. A reflectivity curve from a compressed arachidic acid monolayer on pure water is shown in Figure 3(a) (open circles). The oscillations are indicative of a dense region about 24 Å from the surface: this is attributed to the COOH headgroups, positioned between the water subphase and the hydrocarbon tails which stick up towards the vapor (Figure 4(a), diagram at top). The data are fit (Figure 3(a), solid line) to the calculated reflectivity from a model density profile, which is illustrated in Figure 4(a). Other reflectivity curves and models shown in Figures 3 and 4 correspond to the different calcium carbonate experiments described above, at the time of initial sample preparation (open symbols, blue curves) and also 12 hours later (closed symbols, red curves). We will now discuss the main results from each experiment. Detailed discussions are given in [6] and in manuscripts presently in preparation.

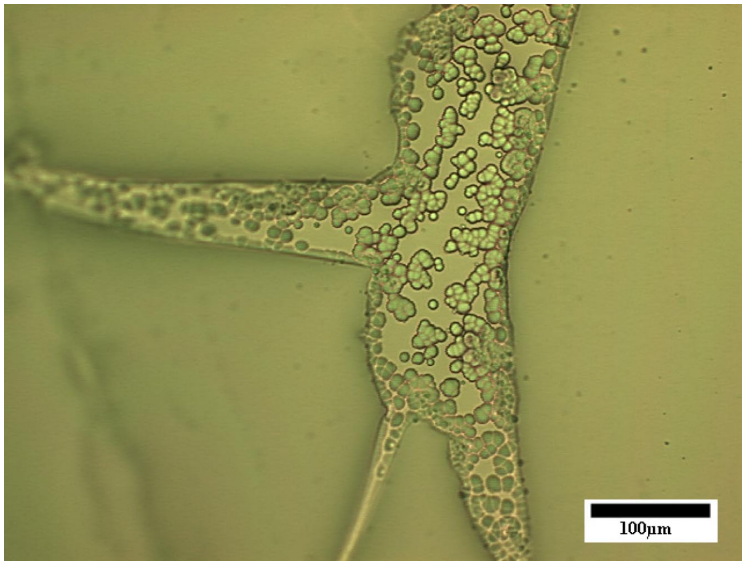

Figure 2. *Optical micrograph through crossed polarizers of a calcite film grown under the conditions of Figure 1(c).*

Data from a monolayer on a diluted calcium bicarbonate subphase, the first scheme illustrated in Figure 1, is shown in Figure 3(b). The maxima are more pronounced than for arachidic acid on pure water. This indicates a greater charge density in the headgroup region, shown by the corresponding model in Figure 4(b). This may be explained by Ca^{2+} ions collecting at the charged headgroups. After a twelve hour interval, the reflectivity is essentially the same, except for being much lower near q=0. This is simply due to homogeneous nucleation of macroscopic calcite crystals from solution, which clutter the surface and interrupt the beam at low incident angles. Grazing incidence diffraction in this case was consistent with hexagonally packed, untilted arachidic acid molecules, accompanied in a few hours' time by resolution limited Bragg peaks from both calcite and vaterite [6]. We found no evidence for Ca^{2+} ordering in-plane, nor for coherently scattering, oriented crystallites as proposed in Figure 1(d). This oriented crystallization cannot be ruled out from our studies, but it has not been directly observed in this rapidly crystallizing system.

Our observations are dramatically different when nucleation is retarded by the presence of acidic macromolecules. The results of adding polyacrylic acid to a supersaturated $CaCO_3$ subphase are shown in Figure 3(c). Again at early times, we observe cation binding at the monolayer. But as the experiment progresses, a sharp peak appears at low q. This peak indicates the formation of a dense mineral layer beneath the surfactant (Figure 4(c)). In fact, we observed this film from its initial thickness of 60 Å to a final thickness of 280 Å, twenty hours later. No in-plane diffraction peaks were observed except those from the arachidic acid, which remained unchanged during mineralization. The amorphous precursor has a density indicative of a hydrated calcium carbonate phase. Only after about twenty hours did Bragg peaks from crystalline $CaCO_3$ begin to appear. In this case, therefore, mineralization occurs as shown in Figure 1(e), via an amorphous precursor that does not strongly interact with the template structure – at least during early stages of nucleation.

The final case of the liquid mineral precursor, promoted by polyaspartic acid and Mg^{2+} ions in solution, is shown in Figure 3(d), with the corresponding model in Figure 4(d). The reflectivity data are similar to the first scheme, with cation binding at the surface but no observable mineral film. However, this experiment is actually very different from the former case because of the localization of the carbonate concentration, which is being pumped into the solution. The liquid mineral precursor did not form a microscopic film, but instead segregated into regions that were soon observable by eye. (These regions were too rough for the surface scattering.) Measurements of the surface pressure in the sample trough showed that the pressure increased

from 12 to 33 mN/m, as if the mineral phase collecting at the surface were pushing the monolayer out of its way. Therefore in this case, the mechanism of nucleation is likely to be that illustrated in Figure 1(f), where we have measured the reflectivity of regions of the monolayer which remained independent of the mineral precursor.

It is quite interesting to compare the proportion of Ca^{2+} ions found at the surface under the different experimental conditions, at the time of sample preparation. For each of these cases, the additional charge density (relative to the case of arachidic acid on pure water) is determined from the model fits. This extra charge is presumed to come from Ca^{2+} and water (never Mg^{2+}, which is more likely than Ca^{2+} to remain solvated [10]), but the proportion will depend upon the volume of water displaced by the cations in the region near the headgroups. We estimate the ratio of cation volume to water molecule volume to be in the range 0.4 to 1.0 (from tabulated Ca^{2+} and H_2O diameters of 2.2 Å and 3.0 Å respectively), and thus calculate the number of arachidic acid molecules per cation from the data. For the diluted $CaCO_3$ subphase of scheme (a), we find one cation per 5 to 9 molecules. These values seem consistent with the fact that at this near-neutral pH, the COOH headgroups should not be significantly ionized. For experimental scheme (b), with polyacrylic acid in an undiluted $CaCO_3$ subphase, the proportion is in the range of 20-35 molecules per cation. Further experiments will be required to determine how this apparent charge depletion depends on the concentration of the polyacrylic acid. In the case of the liquid precursor, scheme (c), the initial subphase contains cations but no carbonate groups. Here the charge collected at the monolayer interface is the largest, in the range of 2-4 molecules per cation. This is the only case where the molecule:cation ratio approaches that required for direct template-matched growth of crystallites at the interface as suggested in [7], yet at this stage the precursor phase is still amorphous.

In conclusion, we have made the first quantitative structural observations of biomimetic mineralizing systems at a Langmuir film interface, from the initial collections of cations to the final macroscopic crystals or films. One question we have addressed concerns mineralization routes through amorphous precursors. We

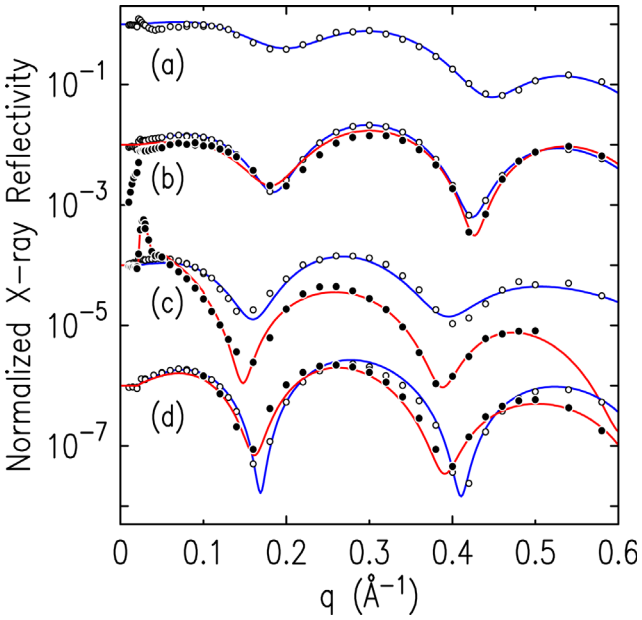

Figure 3. *Fresnel-normalized x-ray reflectivity data (symbols) and fit curves (lines) vs. momentum transfer* q, *for arachidic acid monolayers on different subphases. Open circles are immediately after sample preparation, closed circles show data measured twelve hours later. (a) Pure water. (b) Diluted calcium bicarbonate solution. (c) Supersaturated calcium bicarbonate solution with polyacrylic acid. (d) Ca^{2+} and Mg^{2+} cations in solution, carbonate pumped in. Curves (b) through (d) are shifted for clarity.*

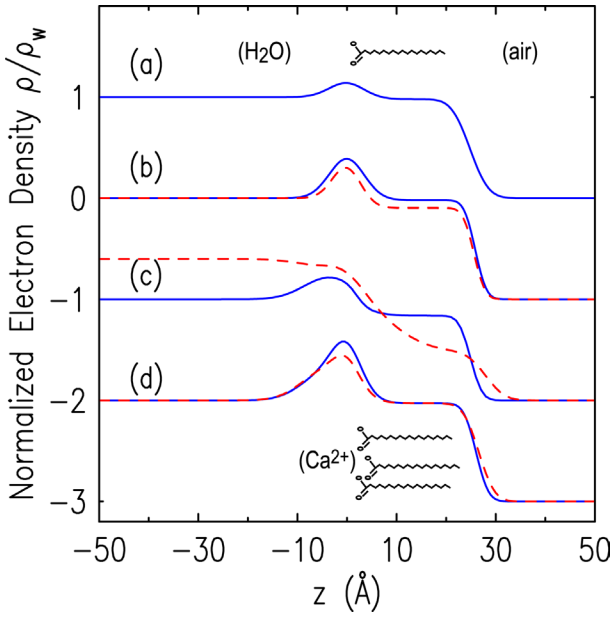

Figure 4. *Normalized electron density of models fit to reflectivity data. Solid lines are immediately after sample preparation, dashed lines are twelve hours later. (a) Arachidic acid on pure water, showing regions in* z *corresponding to the air (z > 30), hydrocarbon tail (0 < z < 30), headgroup (z=0), and water subphase (z < 0). (b) Model profile for monolayer on diluted $CaCO_3$ solution. (c) Supersaturated $CaCO_3$ solution with polyacrylic acid. This system forms an amorphous mineral film that extends for 60-280 Å. (d) Ca, Mg, and polyaspartic acid in subphase. Diagram indicates calcium ion binding. Curves (b) through (d) are shifted for clarity.*

have identified systems that mineralize in this way, and for the first time, we can provide time-dependent structural information: film density, growth rate, dependence of kinetics on polymer concentration, and so on. Studies along these lines should provide considerable new information about how the chemical species present can affect the kinetics of biomineralization. At the same time, we have other objectives which await further experiments. We still have not, we believe, made direct observations of truly template-directed crystal nucleation. While the fundamental question of the interplay between kinetics and the template in biomineralizing systems remains unanswered, we expect synchrotron x-ray scattering to play a significant part in unraveling this question in the future.

Acknowledgments

This work is supported by the Engineering Research Center (ERC) for Particle Science and Technology at the University of Florida, the National Science Foundation (Grant #EEC-94-02989), and the Industrial Partners of the ERC. The NSLS is supported by the U.S. Department of Energy, Division of Materials Sciences and Division of Chemical Sciences, under Contract No. DE-AC02-98CH10886.

References

[1] M. Sarikaya and I. A. Aksay, Results and Problems in Cell Differentiation **19** (1992) 1.
[2] Y. Levi-Kalisman, S. Raz, S. Weiner, L. Addadi, and I. Sagi, J. Chem. Soc. Dalton Trans. (2000) 3977.
[3] J. Aizenberg, J. Hanson, T. F. Koetzke, S. Weiner, and L. Addadi, J. Am. Chem. Soc. **119** (1997) 881.
[4] V.M. Kaganer, H. Möhwald, and P. Dutta, Rev. Mod. Phys. **71** (1999) 779.
[5] J. Daillant, Current Science **78** (2000) 1496.
[6] E. DiMasi and L.B. Gower, Proc. Materials Research Society (in press, 2002).
[7] S. Mann, B.R. Heywood, S. Rajam, and J.D. Birchall, Nature **334** (1988) 692. Note that in this work, a stearic acid monolayer ($CH_3[CH_2]_{16}COOH$) was used.
[8] G. Xu, N. Yao, I. A. Aksay, and J.T. Groves, J. Am. Chem. Soc. **120** (1998) 11977.
[9] L.B. Gower and D.J. Odom, Journal of Crystal Growth **210** (2000) 719.
[10] F. Lippmann, *Sedimentary Carbonate Materials*, Springer-Verlag, NY (1973).